

# Preparation of calcium sulfate dihydrate and calcium sulfate hemihydrate with controllable crystal morphology by using ethanol additive

Zongyou Pan<sup>a,b</sup>, Yi Lou<sup>a,b</sup>, Guangyong Yang<sup>a,b</sup>, Xiao Ni<sup>a</sup>, MoChuan Chen<sup>a</sup>, Huazi Xu<sup>a,\*</sup>,  
Xigeng Miao<sup>c</sup>, Jianli Liu<sup>b</sup>, Chunfeng Hu<sup>b</sup>, Qing Huang<sup>b,\*</sup>

<sup>a</sup>Department of Orthopedic Surgery, Second Affiliated Hospital of Wenzhou Medical College, Wenzhou, Zhejiang 325000, China

<sup>b</sup>Division of Functional Materials and Nanodevices, Ningbo Institute of Materials Technology and Engineering (NIMTE), Chinese Academy of Sciences (CAS), Ningbo, Zhejiang 315201, China

<sup>c</sup>Division of Substrate Development, Department of Fabrication, Kuang-Chi Institute of Advanced Technology, Shenzhen, Guangdong 518000, China

Received 7 November 2012; received in revised form 18 December 2012; accepted 18 December 2012

Available online 4 January 2013

## Abstract

Calcium sulfate hemihydrate (CSH) with controlled crystal morphology has attracted broad interests due to its superior physical and chemical properties, as well as excellent biological performance. In this study, calcium sulfate dehydrate (CSD) was firstly synthesized via the reaction of  $\text{H}_2\text{SO}_4$  and  $\text{Ca}(\text{OH})_2$  using ethanol as morphology modifier. The prepared CSD was then converted to CSH through a hydrothermal method. It was found that the precipitation time of CSD powders was dramatically shortened and the morphology of CSD crystals was changed from thick tabular to short-rod with the increment in ethanol addition. The finally-obtained CSH crystals were found to have hexagonal prisms shape with smaller aspect ratios. The CSH powder with the desired crystal morphology would provide improved setting behavior and biological performance of the CSH bone cement.

© 2012 Elsevier Ltd and Techna Group S.r.l. All rights reserved.

**Keywords:** Bone graft substitute; Calcium sulfate hemihydrate; Crystal morphology; Ethanol additive

## 1. Introduction

Calcium sulfate (CS), an important family of minerals used in laboratory and industry, exists in three forms including dihydrate ( $\text{CaSO}_4 \cdot 2\text{H}_2\text{O}$ , CSD), hemihydrate ( $\text{CaSO}_4 \cdot 0.5\text{H}_2\text{O}$ , CSH) and anhydrite ( $\text{CaSO}_4$ ). Among them, CSH has attracted widespread attentions as one of bone regeneration materials due to the advantages of complete resorption without inflammatory response, excellent osteoconductivity and the ability of promoting bone regeneration and hemostasis [1–6]. Moreover, CSH is a typical cement material. Its self-setting feature allows forming products with desired shapes or complex geometry.

Therefore, CSH has been widely accepted as bone defect filler in clinical operations [7–9].

Numerous researches have focused on the relationship between the properties of CSH and its crystal morphology. The studies on commercial CSH (OsteoSet®) showed that the crystals have a regular prismatic shape with a narrow size distribution. The corresponding material possessed a slow, predictable re-absorption and superior biological performance [10–12]. Equiaxed CSH crystals having low aspect ratios were also synthesized by Peng et al. to enhance its injectability and mechanical properties [13]. Woo et al. evaluated the mechanical and handling properties, and biological performances of CSH with different crystal structures [14]. They demonstrated that of the crystal structure of CSH determined its mechanical properties for supporting the osteoblast differentiation. Thus, for clinic applications, it is meaningful to develop a methodology to prepare high-grade CSH with controlled morphology and grain size [15–17].

\*Corresponding authors.

E-mail addresses: [spinexu@163.com](mailto:spinexu@163.com) (H. Xu),  
[huangqing@nimte.ac.cn](mailto:huangqing@nimte.ac.cn) (Q. Huang).

Two methods are commonly employed to prepare CSH. One is the dehydration of the CSD precursor at elevated temperatures and pressures [18,19]. The other is the hydrothermal method, in which CSD precursor was treated in boiling solutions of inorganic acids or salts (such as  $\text{H}_2\text{SO}_4$ ,  $\text{KCl}$ ,  $\text{CaCl}_2$  and  $\text{MgCl}_2$ ) under atmospheric pressure to synthesize high-grade CSH [20–23]. The hydrothermal method is more economic and moderate for the mass production of CSH with good repeatability. Some organic reagents can inhibit or promote the grain growth along particular crystallographic planes to modify the crystal morphology. E.g., ethanol could effectively affect the shape and size of the  $\text{CaCO}_3$  nanoparticles prepared by the hydrothermal method [24–26]. Since  $\text{CaCO}_3$  and  $\text{CaSO}_4$  have similar polar crystallographic planes which would be interacted by the modifying reagent, it is reasonable to try ethanol to control the morphology and size of CSH crystals which is crucial for bone graft substitute.

In this study, we firstly prepared CSD through the reaction between  $\text{Ca}(\text{OH})_2$  and  $\text{H}_2\text{SO}_4$  in a water/ethanol mixture using a precipitation method. Ethanol was used as a morphology modifier reagent to control the final morphology of CSD crystals. The hydrothermal method was then used to dehydrate the as-prepared CSD to obtain final CSH product. The effect of ethanol on the morphologies of CSD and CSH crystals were comprehensively investigated, and the underlying mechanism was tentatively discussed based on the crystal-plane-selective-absorption characteristic of ethanol molecules.

## 2. Experimental procedures

### 2.1. Materials

All chemicals used in this study were of analytical grade and produced by the Sinopharm Chemical Reagent Co. Ltd. (Shanghai, China). Concentrated Sulfuric acid was diluted to a 1.2 mol/L  $\text{H}_2\text{SO}_4$  solution. 99.7 wt% absolute ethanol was used as the morphology modifier. A 30 wt%  $\text{CaCl}_2$  solution was used as the medium for the conversion of CSD precursor to final CSH product.

### 2.2. Methods

The precipitation process of CSD is described as follows. Firstly, ethanol/water solutions with various ethanol/water volume ratio (R) ranging from 0 to 4:3 were prepared and stirred by magnetic stirring for 30 min. Then,  $\text{Ca}(\text{OH})_2$  was dissolved in the ethanol/water solution to form a saturated solution followed by titration of  $\text{H}_2\text{SO}_4$  solution. The obtained suspension was kept stirred for 4 h to ensure a complete reaction. After that, the CSD precipitate was centrifuged at 3000 rpm for 10 min and dried at 40 °C for 30 min in oven.

A hydrothermal method was used to dehydrate the as-prepared CSD precursor to final CSH product. A 30 wt%  $\text{CaCl}_2$  solution was added into a three-neck flask equipped with a reflux condenser and kept in an oil bath at 110 °C. Then, the as-prepared CSD powders were added into the

boiled solution and stirred for 6 h. After that, the prepared CSH powders were quickly filtered and then dried at 110 °C for 30 min in oven.

### 2.3. Characterization

The precipitation process of CSD powders was carefully monitored. The onset of precipitation was determined as the obvious precipitation phenomenon occurred (a cloudy white precipitate appeared in the transparent reaction solution).

The morphology and the phases composition of the as-prepared CSD and CSH powders were examined using a field emission scanning electron microscopy (FE-SEM; S-4800, Hitachi Science System Ltd., Japan) and X-ray diffraction (XRD; D8 Advance, Bruker Inc., Germany), respectively. The XRD analysis was performed with  $\text{CuK}\alpha$  radiation at a scanning rate of 1°/min in the 2 $\theta$  range from 10° to 40°. The particle size of the CSD was measured by a laser particle size analyzer (Microtra S3500, A Unit of Nikkiso Co. Ltd., Tokyo, Japan) after ultrasonic treatment in the anhydrous ethanol solution. The grain size and the average aspect ratio of CSH crystals were analyzed on the basis of the SEM data.

### 2.4. In vitro biocompatibility

Assessments of cytotoxicity were carried out according to ISO 10993-5 [27,28] using an extraction method with mouse fibroblast cell line L929. The extracts were prepared as follows: CSH powders were added to Dulbecco's Modified Eagle's Medium (DMEM; Gibco, USA) and kept in a humidified atmosphere of 5%  $\text{CO}_2$  at 37 °C for 24 h. The ratios of powder weight to medium volume were ranging from 25 mg/ml to 200 mg/ml. After incubation, the mixture was centrifuged to collect the supernatant.

The cell suspension with a density of  $3 \times 10^3$  cell/ml was prepared. 100  $\mu\text{l}$  cell suspension was added to the wells of the 96-well plate and incubated for 24 h to allow attachment. Then the culture media were replaced by 50  $\mu\text{l}$  of extracts and 50  $\mu\text{l}$  of DMEM with 20% fetal calf serum (FCS). The DMEM with 10% FCS was used as negative control. A cell counting kit-8 (CCK 8; Dojind Molecular Technologies Inc., Japan) was employed to quantitatively evaluate the cell viability as follows: after incubating for 1, 3 and 5 days, each well was added with 10  $\mu\text{l}$  of 5 mM 2-(2-methoxy-4-nitrophenyl)-3-(4-nitrophenyl)-5-(2,4-disulfophenyl)-2 H tetrazolium monosodium salt (WST-8) and cultured for 2 h. The optical density (OD) of each well at 450 nm was measured by a microplate reader (Infinite M200 Pro, Tecan Group Ltd., Switzerland). Six samples per group were tested.

## 3. Results

### 3.1. Influence of ethanol concentration on the precipitation of calcium sulfate dihydrate (CSD)

The effect of ethanol on the CSD precipitation was evaluated by the onset time of precipitation. Table 1

summarizes the onset time for CSD precipitation in solutions with various  $R$  from 0 (no ethanol) to 4:3. The reaction time as long as  $48 \pm 3$  h is required to initiate the CSD precipitation in pure aqueous solutions ( $R=0$ ) because of the low solubility of  $\text{Ca}(\text{OH})_2$  (0.173 g/100 mL at 20 °C) in water. The thus low concentration of  $\text{Ca}^{2+}$  ion can not meet the requirement that a supersaturation condition of  $\text{Ca}^{2+}$  is needed to precipitate CSD. With the addition of ethanol, however, the precipitation times were remarkably shortened. Specifically, the precipitation onset time was reduced to 3 min when  $R$  reached 1. Further addition of ethanol showed no visible change on the onset time of precipitation. The accelerated precipitation due to the addition of ethanol is meaningful to improve the yield of CSD precursor.

Table 1

The onset times of the CSD precipitation in ethanol/water solutions with various ethanol/water volume ratios.

Ethanol/water volume ratios	0	1:3	2:3	1:1	4:3
The onset times	$48 \pm 3$ h	$15 \pm 3$ min	$5 \pm 1$ min	$3 \pm 1.1$ min	$2 \pm 0.6$ min

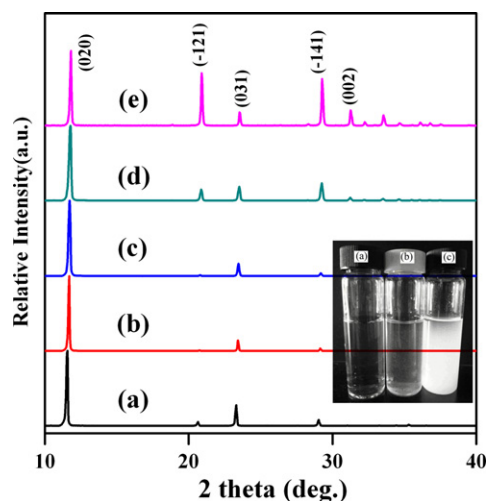


Fig. 1. X-ray diffraction patterns of the calcium sulfate dihydrate (CSD) synthesized at ethanol/water ratios ( $R$ , v/v) of (a) 0; (b) 1:3; (c) 2:3; (d) 1:1 and (e) 4:3. The inset depicts the starting reaction solution (a) and the final state of solution after 48 h reaction without (b) and with ethanol when  $R$  is 1:1 (c) showing the largely improved yield of CSD product.

Table 2

Indexation results of the X-ray diffraction patterns of the CSD synthesized at various ethanol/water volume ratios.

Ethanol/water volume ratios	$\theta$ (deg.)				$d$ (Å)				Lattice parameters (Å)/(deg.)			
	020	–121	031	–141	020	–121	031	–141	$a$	$b$	$c$	$\beta$
1:3	5.831	10.375	11.703	14.567	7.582	4.278	3.798	3.063	5.672	15.164	6.540	118.3
2:3	5.863	10.414	11.733	14.599	7.542	4.262	3.788	3.056	5.670	15.083	6.525	118.3
1:1	5.865	10.426	11.743	14.609	7.539	4.257	3.785	3.054	5.658	15.078	6.517	118.3
4:3	5.883	10.438	11.764	14.630	7.516	4.252	3.778	3.050	5.655	15.032	6.515	118.3

Fig. 1 shows the XRD patterns of CSD powders prepared in water ( $R=0$ ) and ethanol/water mixture solutions with different  $R$  ranging from 1:3 to 4:3. All peaks were indexed corresponding to calcium sulfate dihydrate phase (JCPDS card 74–1433) with the monoclinic structure, indicating a fully crystallized CSD phase. The calculated crystallography data based on a monoclinic lattice of CSD are also listed in Table 2. It is found that all the diffraction peaks of CSD synthesized in mixture solutions shift slightly to higher  $2\theta$  values with the increment of the ethanol, indicating the reduced  $d$ -spacing of lattice and compacted lattice volume in the as-prepared CSD crystal modified by ethanol during synthesis. The calculated lattice parameters further present that a higher  $R$  led to smaller lattice parameters in the products. The inserted photo in Fig. 1 shows the starting reaction solution (marked a), CSD product in the solutions without (marked b) and with ethanol addition ( $R=1$ , marked c) after 48 h reaction. It is obvious that the production yield of CSD without the ethanol is negligible and the solution is nearly as transparent as the starting solution. Actually, it has been experimentally proven that even after a prolonged duration (72 h) the yield of CSD product in the water solution was still extremely low that the powder was hard to be collected for the further dehydration reaction to synthesize CSH crystal. However, the addition of ethanol in the reaction solution largely accelerated the reaction process and the productivity of CSD product was almost 100%.

The crystal morphology and size distribution of CSD were analyzed by SEM (see Fig. 2). It can be seen that the typical crystal morphology of CSD produced when  $R$  is 1:3 is plate-like (Fig. 2a) that is much similar to that produced in the water solution without ethanol (shown in the inserted image in Fig. 2a). When  $R$  reaches 2:3 and 1:1, rod and thick plate-like crystals with reduced dimension could be obtained, as shown in Fig. 2b and c. At the highest  $R$  of 4:3 in current experiment, most of CSD crystals are typically short rod-like and had an average aspect ratio of 4 (Fig. 2d). Obviously, the addition of ethanol was very effective to modify the dimensions of CSD crystals.

### 3.2. Influence of ethanol concentration on the preparation of calcium sulfate hemihydrate (CSH)

The XRD results of the as-prepared CSH powders are shown in Fig. 3. It confirms that the CSD precursors had

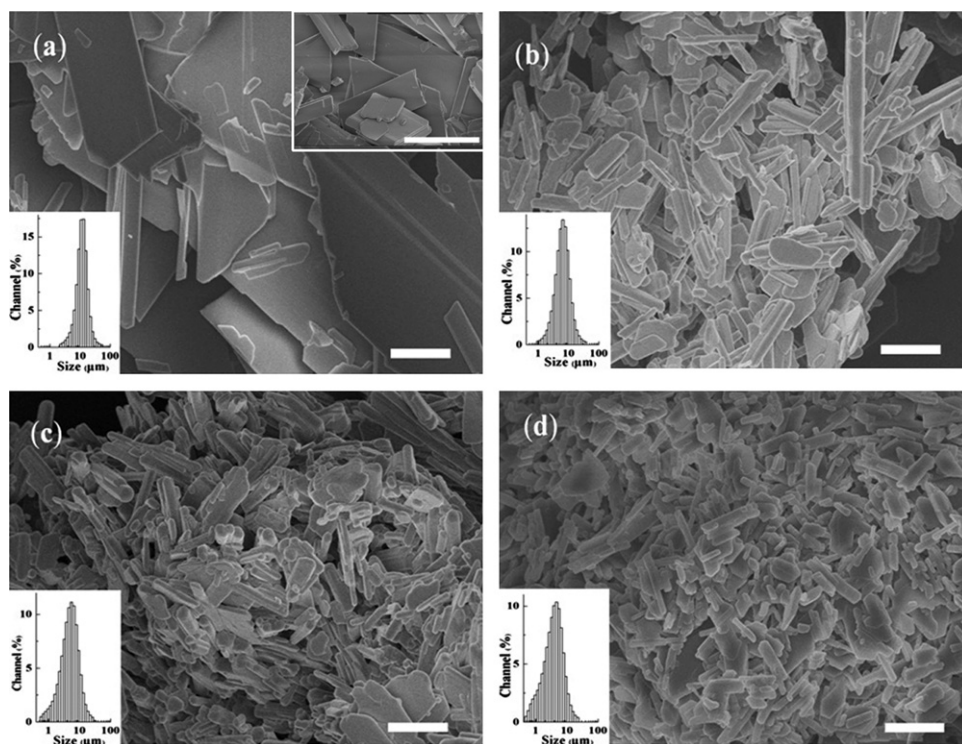


Fig. 2. Scanning electron microscopy images of the calcium sulfate dehydrate (CSD) synthesized at ethanol/water ratios ( $R$ , v/v) of (a) 1:3; (b) 2:3; (c) 1:1 and (d) 4:3. The inset in (a) shows the morphology of CSD produced in water solution. The scale bars are 4  $\mu\text{m}$ .

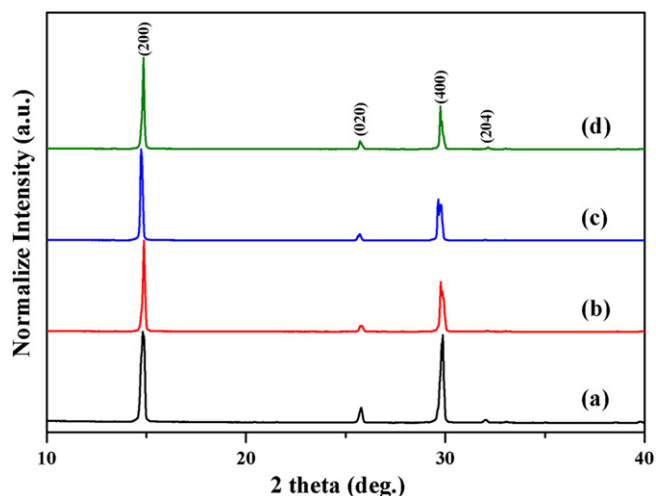


Fig. 3. X-ray diffraction patterns of the calcium sulfate hemihydrates (CSH) prepared from calcium sulfate hydrate (CSD) synthesized at ethanol/water ratios ( $R$ , v/v) of (a) 1:3; (b) 2:3; (c) 1:1 and (d) 4:3.

been completely converted into CSH phase (JCPDS card 81-1848) with a hexagonal crystal structure.

SEM images of the as-prepared CSH crystals are shown in Fig. 4a–d. The length distributions of the CSH crystals are also plotted in the inserted histogram graphs. It can be seen that the CSH grains were typical hexagonal prism. As  $R$  increased from 1:3 to 4:3, the dimensions of resultant CSH crystals were significantly reduced. The mean length and width of the CSH crystals decrease from  $52 \pm 11.3 \mu\text{m}$  to

$17 \pm 3.4 \mu\text{m}$  and from  $13 \pm 2.5 \mu\text{m}$  to  $8 \pm 1.6 \mu\text{m}$ , respectively. Correspondingly, the average aspect ratio decreases from 4.0 to 2.1. Meanwhile, hexagonal prism crystals became more homogeneous with a higher crystallinity. At  $R=4:3$ , the obtained CSH crystals have a fine and uniform morphology as shown in Fig. 4d. Table 3 summarizes the statistic dimensions of CSH crystals according to the SEM analysis. It is obvious that ethanol was an effective reagent for controlling the morphology and the size distribution of CSH crystals.

### 3.3. *In vitro* biocompatibility of the as-prepared calcium sulfate hemihydrate

In order to fully evaluate the *in vitro* biocompatibility of the as-prepared CSH products, CSH powders derived from the CSD synthesized at  $R=1:3$  and  $4:3$  were selected. The OD values detected from the CCK-8 assay provide an indication of cell growth and proliferation in the extracts of CSH powders. As shown in Fig. 5, the proliferation of L929 cells in CSH extracts showed the same level as that in blank control sample regardless of the extract concentration and the culture period (1, 3, 5 days in current experiment). Meanwhile, the CSH product derived from CSD precursor prepared at high  $R$  value shows much better biocompatibility than that derived from CSD precursor prepared at low  $R$  value. It was indicated that the obtained CSH powders did not display significant cytotoxicity against cells.



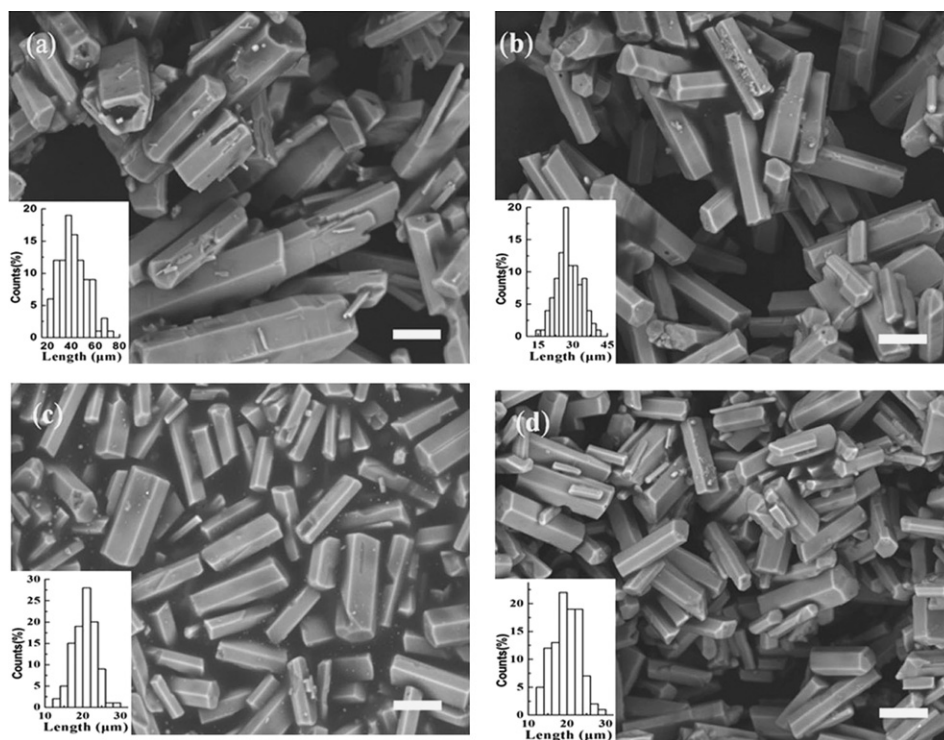


Fig. 4. Scanning electron microscopy images of the calcium sulfate hemihydrate (CSH) derived from calcium sulfate hydrate (CSD) synthesized at ethanol/water ratios ( $R$ , v/v) of (a) 1:3; (b) 2:3; (c) 1:1 and (d) 4:3. The scale bars are 10  $\mu\text{m}$ .

Table 3

Dimensions of the CSH prepared from CSD synthesized at various ethanol/water volume ratios.

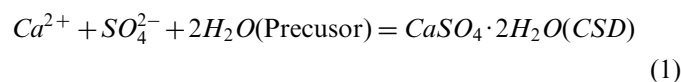
Ethanol/water volume ratios	1:3	2:3	1:1	4:3
Length ( $\mu\text{m}$ )	$52 \pm 11.3$	$28 \pm 5.2$	$21 \pm 2.9$	$17 \pm 3.4$
Width ( $\mu\text{m}$ )	$13 \pm 2.5$	$10 \pm 1.6$	$9 \pm 1.3$	$8 \pm 1.6$
Aspect ratio	4	2.8	2.3	2.1

## 4. Discussion

### 4.1. Influence of ethanol additive on the thermodynamic of calcium sulfate dihydrate (CSD)

The acceleration of the precipitation of CSD by adding ethanol could be explained in terms of kinetics of the precipitation reaction, including the nucleation and crystal growth rate, the supersaturation condition and the solvent (ethanol) in the solution.

A liquid–solid equilibrium between  $\text{Ca}^{2+}$ ,  $\text{SO}_4^{2-}$  ions and the  $\text{CaSO}_4 \cdot 2\text{H}_2\text{O}$  solid phase took place during the CSD precipitation, i.e.



Thus, the supersaturation ( $S$ ) could be expressed by:

$$S = \frac{K_{sp}}{\alpha_{\text{Ca}^{2+}} \alpha_{\text{SO}_4^{2-}} \alpha_{\text{H}_2\text{O}}^2} \quad (2)$$

where  $K_{sp}$  is the thermodynamic equilibrium constant of CSD, which is only a function of temperature.  $\alpha_i$  is the activity of the corresponding species. Because  $K_{sp}$  is a constant at the defined experimental temperature, it can be seen that the supersaturation  $S$  during CSD precipitation is determined by the water activity ( $\alpha_{\text{H}_2\text{O}}$ ). It has been proven that ethanol in an aqueous solution decreased the  $\alpha_{\text{H}_2\text{O}}$  [32,33]. Therefore, the increase of ethanol concentration will result in a higher supersaturation in solution, which accelerates the nucleation kinetics of reaction. The high supersaturation induced by the increasing ethanol concentration could also provide a high drive force for the incorporation of  $\text{Ca}^{2+}$  and  $\text{SO}_4^{2-}$  ions into CSD crystal lattice, which will promote the following crystal growth.

It can be seen from the previous section that both shapes and sizes of synthesized CSD particles changed upon the addition of ethanol. Such facts imply that the addition of ethanol resulted in not only a fast precipitation of the CSD particles but also a uniform morphology. It demonstrates that the ethanol acted as an effective surfactant to prepare CSD particles, which is in good agreement with the results of different materials [34,35]. The addition of ethanol changes the chemical properties of the solvent in the supersaturation of CSD, such as the dielectric constant of the medium, ion inter-attraction and the solute–solvent interaction as a result of the solubility difference, which could have significant effect on the crystal formation and growth [36].

Moreover, ethanol can modify the surface energies of specific crystal planes. It is well known that  $\text{Ca}^{2+}$  is coordinated by six sulfate oxygen atoms and two water

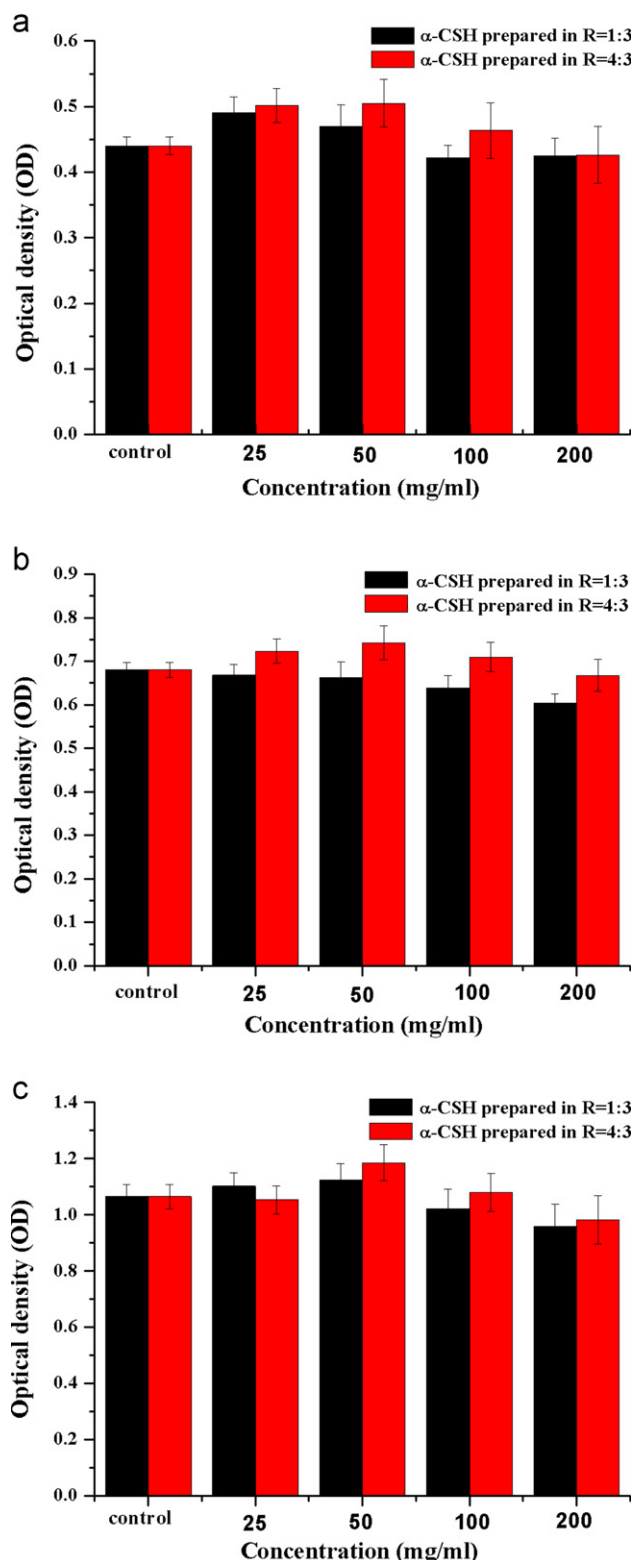


Fig. 5. Cell proliferation in the presence of the dissolution extracts of calcium sulfate hemihydrate (CSH) derived from calcium sulfate hydrate (CSD) synthesized at the ethanol/water ratios ( $R$ , v/v) of 1:3 and 4:3 for different periods. (a) 1 day, (b) 3 days, (c) 5 days.

molecules along the  $c$ -axis in CSD, as depicted in Fig. 6a. At different directions of the crystal axis, the differences in bond types and bond energies between  $\text{Ca}^{2+}$  and  $\text{SO}_4^{2-}$  ions

result in different growth rates of crystal planes. Fig. 6b demonstrates a typical monoclinic CSD crystal showing the habit crystal planes. Crystal growth rates of the crystal planes along three directions are ordered as follows:  $\{111\} > \{110\} > \{010\}$ .  $\{111\}$  planes are occupied by  $\text{Ca}^{2+}$  while  $\{110\}$  planes are composed of  $\text{Ca}^{2+}$  and  $\text{SO}_4^{2-}$  ions. Without ethanol addition, the crystal grows faster along the  $c$  axis than along  $a$  and  $b$  axes, and  $\{111\}$  planes having high surface energy tend to disappear, therefore the final CSD shows the plate-like crystals. After adding ethanol, ethanol tends to selectively adsorb on the CSD grain surface by substituting of the water molecules. Such calcium–ethanol interactions are shown schematically in Fig. 6c and d. The OH group of the ethanol absorbed on the surface of the CSD crystal may form a bond with  $\text{Ca}^{2+}$  at  $\{111\}$  planes, which decreases the surface energy and thus balances the growth rates along different planes during crystallization. It is obvious that the morphology of ethanol-modified CSD particles gradually transform from needle-like to final rod-like in contrast with plate-like shape of pristine CSD crystals (Fig. 2), indicating that the surface energy at basal plane and prismatic planes becomes indistinguishable.

#### 4.2. Influence of ethanol additive on the morphology and size distribution of calcium sulfate hemihydrate (CSH) powders

The transition from CSD precursor to final CSH is reported to be two-step process: dissolution of CSD precursor and re-precipitation or recrystallization of CSH phase [38]. As discussed above, the ethanol adsorbed on CSD surface can inhibit the crystal growth along  $[111]$  and  $[110]$  directions. As a result, the surface area of polar plane  $\{111\}$  becomes comparable to that of prismatic planes such as  $\{110\}$  and  $\{010\}$ . It can be deduced that  $\text{Ca}^{2+}$  and  $\text{SO}_4^{2-}$  ions concentrations variation during dissolution of CSD is highly dependent on the crystal planes. Since  $\{111\}$  planes are intrinsically in a high energy state, the release rate of  $\text{Ca}^{2+}$  and  $\text{SO}_4^{2-}$  ions will be accelerated in the ethanol-modified rod-like CSD precursor (ethanol bonding on the surface that proposed in the formation of CSD crystal will be eliminated soon in the salt solution). Thus, high concentration of ions (especially  $\text{SO}_4^{2-}$  ion) locally promotes the nucleation of CSH crystal, and consequently the increase of density of nuclei promotes the formation of equiaxed crystals. Therefore, the short rod-like CSH grains were obtained, instead of the common needle or fiber-like shapes.

The morphology control of CSH crystal is important to determine the following self-setting and compressive strength of CSD cement when it is mixed with water as bone cement. Wang et al. reported that through treating in the  $\text{CaCl}_2$  solution of various concentrations, the CSH morphology can be modified from long-and-slim hexagonal rods with an aspect ratio of 5.5 to fat-and-short hexagonal columns with an aspect ratio of 1.4, and the low aspect ratio sample showed a much higher compressive strength (37 MPa) [13]. The self-setting behavior of CSH makes it one of the candidate bone cements for bone augmentation. The hydration of hemihydrate does not

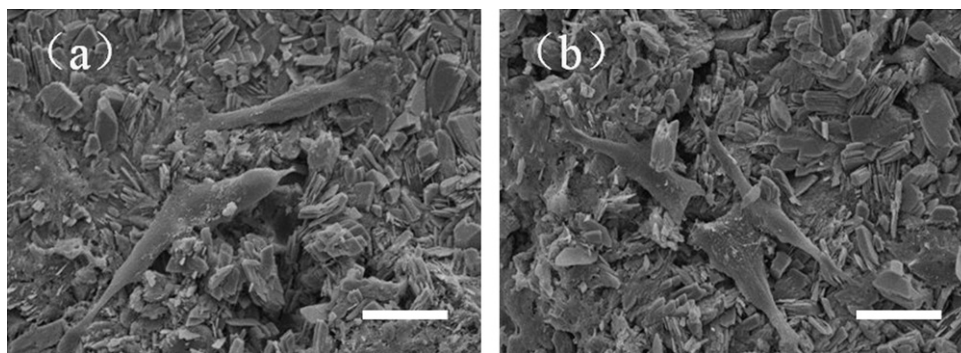


Fig. 6. (a) View of a calcium sulfate hydrate (CSD) crystal along the *c*-axis, showing the calcium-coordinated water molecules; (b) Schematic drawing of a monoclinic calcium sulfate hydrate (CSD) crystal; (c), (d) Possible interactions of ethanol with the calcium sulfate hydrate (CSD) surface. Color codes: calcium: blue, sulfate: yellow, oxygen: red, hydrogen: pink.

only depend on intrinsic crystal property but also related to the crystallization habit at different crystal planes [39–41]. Lewry et al. have revealed that the setting behavior of CSH was closely related to the shape and size of the CSH crystals [39]. CSH with a lower aspect would provide more nucleation sites for the crystallization of gypsum. The fast setting behavior of CSH due to its modified crystallographic microstructures, equiaxial microstructure is preferred for the dissolution of CSH and accelerated crystallization of CSD phase. The ethanol addition in the current study to prepare CSD precursor also played the role to shorten the aspect ratio of CSH crystal as indicated in Table 3, and it would also influence the compressive strength of bone cement after hydration (to form CSD bulk). The more detail evaluation of mechanical property is undergoing and will be reported elsewhere.

## 5. Conclusions

In this study, we developed a new methodology to prepare CSD and CSH powders with well controllable morphologies and particle size distribution by using ethanol as the modifying reagent. The addition of ethanol led to a fast precipitation and high yield of CSD. The resulted CSD and CSH have a smaller particle size and more homogeneous distribution of grains with a short-rod shape. It is believed that ethanol can decrease the water activity in the reaction and lead to a larger supersaturation of ions in the solution during the CSD precipitation process. The selective adsorption of the ethanol molecules on the specific crystal surface of CSD resulted in the crystal with rod-like shape and small length/width aspect ratio. The resultant CSD product enabled the synthesis of fine CSH crystal with equal-axial morphology. In the biocompatibility experiment, no major deleterious or cytotoxic responses were observed in as-prepared CSH. Such CSH powders were expected to have better flow ability and self-setting behavior for surgical applications.

## Acknowledgment

This work is supported by the Zhejiang provincial open foundation of the most important subjects (2011GK002),

Zhejiang Provincial Science and Technology Program of China (No. 2011C23113), Zhejiang Bud Talent Plan (2012R413050) and Ningbo Natural Science Fund (2012A610101).

## References

- [1] K.M. Woo, B. Yu, H.M. Jung, Y.K. Lee, Comparative evaluation of different crystal-structured calcium sulfates as bone-filling materials, *Journal of Biomedical Materials Research Part B: Applied Biomaterials* 91 (2009) 545–554.
- [2] J.C. Yang, H.D. Wu, N.C. Teng, D.Y. Ji, S.Y. Lee, Novel attempts for the synthesis of calcium sulfate hydrates in calcium chloride solutions under atmospheric conditions, *Ceramics International* 38 (2012) 381–387.
- [3] B.K. Tay, W. Patel, D.S. Bradford, Calcium sulfate- and calcium phosphate-based bone substitutes, *The Orthopedic Clinics of North America* 30 (1999) 615–623.
- [4] S. Gitelis, P. Piasecki, T. Turner, W. Haggard, J. Charters, Use of a calcium sulfate-based bone graft substitute for benign bone lesions, *Orthopedics* 4 (2001) 162–166.
- [5] Y. Murashima, G. Yoshikawa, R. Wadachi, N. Sawada, H. Suda, Calcium sulphate as a bone substitute for barious osseous defects in conjunction with apicectomy, *International Endodontic Journal* 35 (2002) 768–774.
- [6] A. Scarano, F. Carinci, E. Cimorelli, M. Quaranta, A. Piattelli, Application of calcium sulfate in surgical-orthodontic treatment of impacted teeth: a new procedure to control hemostasis, *Journal of Oral and Maxillofacial Surgery: Official Journal of the American Association of Oral and Maxillofacial Surgeons* 68 (2010) 964–968.
- [7] M.V. Thomas, D.A. Puleo, Calcium sulfate: properties and clinical applications, *Journal of Biomedical Materials Research Part B: Applied Biomaterials* 88 (2009) 597–610.
- [8] R. Mirzayan, V. Panossian, R. Avedian, D.M. Forrester, L.R. Menendez, The use of calcium sulfate in the treatment of benign bone lesions, *Journal of Bone and Joint Surgery American volume* 83 (2001) 355–358.
- [9] I.H. Lieberman, D. Togawa, M.M. Kayanja, Vertebroplasty and kyphoplasty: filler materials, *Spine Journal* 5 (2005) 305–316.
- [10] A. Kutkut, S. Andreana, Medical-grade calcium sulfate hemihydrate in clinical implant dentistry: a review, *Journal of Long-Term Effects of Medical Implants* 20 (2010) 295–301.
- [11] S.N. Parikh, Bone graft substitutes: past, present, future, *Journal of Postgraduate Medicine* 48 (2002) 142–148.
- [12] D.A. Randolph, J.L. Negri, T.R. Devine, S. Gitelis, Controlled dissolution pellet containing calcium sulfate, U.S. Patent (1997) US5614206.
- [13] P. Wang, E.J. Lee, C.S. Park, B.H. Yoon, D.S. Shin, H.E. Kim, Y.H. Koh, S.H. Park, Calcium sulfate hemihydrate powders with a

- controlled morphology for use as bone cement, *Journal of the American Ceramic Society* 91 (2008) 2039–2042.
- [14] K.M. Woo, B. Yu, H.M. Jung, Y.K. Lee, Comparative evaluation of different crystal-structured calcium sulfates as bone-filling materials, *Journal of Biomedical Materials Research Part B: Applied Biomaterials* 91B (2009) 545–554.
- [15] A.J. Lewry, J. Williamson, The setting of gypsum plaster. Part I: the hydration of calcium sulfate hemihydrate, *Journal of Materials Science* 29 (1994) 5279–5284.
- [16] N.B. Singh, B. Middendorf, Calcium sulphate hemihydrate hydration leading to gypsum crystallization, *Prog. Cryst. Growth Charact. Mat.* 53 (2007) 57–77.
- [17] M.J. Ridge, Mechanism of setting of gypsum plaster, *Reviews of Pure and Applied Chemistry* 10 (1960) 243–276.
- [18] B.E.C. Combe, D.C. Smith, Studies on the preparation of calcium sulphate hemihydrate by an autoclave process, *Journal of Applied Chemistry* 18 (1968) 307–312.
- [19] Y.B. Ling, G.P. Demopoulos, Preparation of  $\alpha$ -calcium sulfate hemihydrate by reaction of sulfuric acid with lime, *Industrial and Engineering Chemistry Research* 44 (2005) 715–724.
- [20] X.Y. Song, S.X. Sun, W.L. Fan, H.Y. Yu, Preparation of different morphologies of calcium sulfate in organic media, *Journal of Materials Chemistry* 13 (2003) 1817–1821.
- [21] H.U. Hummel, D. Freyer, J. Schneider, The effect of additives on the crystalline morphology of alpha calcium sulfate hemihydrate: experimental findings and molecular simulations, *Zement Kalk Gips International* 56 (2003) 61–69.
- [22] H. Guan, X.F. Ma, Z.B. Wu, Crystallization routes and metastability of  $\alpha$ -calcium sulfate hemihydrate in potassium chloride solutions under atmospheric pressure, *Journal of Chemical and Engineering Data* 54 (2009) 719–725.
- [23] A. Zürz, I. Odler, F. Thiemann, K. Berghofer, Autoclave-free formation of  $\alpha$ -hemihydrate gypsum, *Journal of the American Ceramic Society* 74 (1991) 1117–1124.
- [24] Q. Li, Y. Ding, F.Q. Li, B. Xie, Y.T. Qian, Solvothermal growth of vaterite in the presence of ethylene glycol, 1,2-propanediol and glycerol, *Journal of Crystal Growth* 236 (2002) 357–362.
- [25] S.R. Dickinson, K.M. McGrath, Polymorphism and morphology of calcium carbonate precipitated in mixed solvents of ethylene glycol and water, *Journal of Materials Chemistry* 13 (2003) 928–933.
- [26] E.M. Flaten, M. Seiersten, J.P. Andreassen, Polymorphism and morphology of calcium carbonate precipitated in mixed solvents of ethylene glycol and water, *Journal of Crystal Growth* 311 (2009) 3533–3538.
- [27] C. Pittet, J. Lemaitre, Mechanical characterization of brushite cements: a Mohr circles' approach, *Journal of Biomedical Materials Research Part B: Applied Biomaterials* 53 (2000) 769–780.
- [28] Z. Huan, J. Chang, Self-setting properties and in vitro bioactivity of calcium sulfate hemihydrate–tricalcium silicate composite bone cements, *Acta Biomaterialia* 3 (2007) 952–960.
- [32] E.T.M.J. Martynowicz, G.J. Witkamp, G.M.V. Rosmalen, The effect of aluminium fluoride on the formation of calcium sulfate hydrates, *Hydrometallurgy* 41 (1996) 171–186.
- [33] F. Göllés, Examination and calculation of thermodynamic data from experimental measurements. I. The numerical integration of the vapor-pressure curves of the system methanol–water, *Monatshefte Fur Chemie* 92 (1961) 981–991.
- [34] F. Göllés, Examination and calculation of thermodynamic data from experimental measurements. II. The numerical integration of the vapor-pressure curves of the system methanol–water, *Monatshefte Fur Chemie* 93 (1962) 191–220.
- [35] H. Gharibi, B.M. Razavizadeh, A.A. Rafati, Electrochemical studies associated with the micellization of dodecyltrimethyl ammonium bromide (DOTAB) in aqueous solutions of ethanol and 1-propanol, *Colloids and Surfaces A* 136 (1998) 123–132.
- [36] F. Manoli, E. Dalas, Spontaneous precipitation of calcium carbonate in the presence of ethanol, isopropanol and diethylene glycol, *Journal of Crystal Growth* 218 (2000) 359–364.
- [38] D. Freyer, W. Voigt, Crystallization and phase stability of  $\text{CaSO}_4$  and  $\text{CaSO}_4$ -based salts, *Monatshefte Fur Chemie* 134 (2003) 693–719.
- [39] A.J. Lewry, J. Williamson, The setting of gypsum plaster: Part III the effect of additives and impurities, *Journal of Materials Science* 29 (1994) 6085–6090.
- [40] Q.Q. Ye, B.H. Guan, W.B. Lou, L. Yang, B. Kong, Effect of particle size distribution on the hydration and compressive strength development of  $\alpha$ -calcium sulfate hemihydrate paste, *Powder Technology* 207 (2011) 208–214.
- [41] N.B. Singh, B. Middendorf, Calcium sulphate hemihydrate hydration leading to gypsum crystallization, *Progress in Crystal Growth and Characterization of Materials* 53 (2007) 57–77.